Contr. Mineral. and Petrol. 14, 321—342 (1967)

Serpentinization at Burro Mountain, California*

NORMAN J. PAGE

Received January 1, 1967

Contents

Abstract. The Burro Mountain ultramafic complex, Monterey County, California, consists of dunites and peridotites which are partially or wholly serpentinized. Primary minerals in both rock types are olivine, enstatite, diopside, and picotite which upon alteration yield chrysotile, lizardite, brucite, magnetite, talc, tremolite, and carbonate. Electron microprobe analyses show that enstatite, $En_{85.8}$ to $En_{90.8}$, alters to "bastite" composed only of lizardite (5.0—12.0 weight percent FeO), whereas olivine, $Fo_{90.8}$ to $Fo_{91.6}$, forms lizardite+chrysotile+brucite with or without magnetite. The chrysotile ranges from 3.0 to 5.0 weight percent FeO, the brucite from 16.0 to 43.0 weight percent FeO. As serpentinization proceeds, the alteration products are enriched in FeO relative to MgO.

Serpentinization probably originates in a changing P_{O_2}-T environment by two different reactions:

(a) Olivine+enstatite+H_2O+O_2 $\rightleftarrows$ Mg, Fe^{+2} chrysotile+Mg, Fe^{+3}, Fe^{+2} lizardite with or without magnetite.

(b) Olivine+H_2O+O_2 $\rightleftarrows$ Fe^{+2}, Mg brucite+Mg, Fe^{+2} chrysotile+Mg, Fe^{+2}, Fe^{+3} lizardite with or without magnetite.

The presence of $Fe(OH)_2$ in brucite indicates that temperatures of serpentinization may be lower than temperature heretofore inferred. This is suggested by thermodynamic calculations, assuming ideal solid solution, and relating the substitution of Fe^{+2} for Mg^{+2} in brucite to the stability field of brucite.

Introduction

The Burro Mountain area in southern Monterey County, California, (Fig. 1) contains a well-exposed example of an "Alpine-type" ultramafic mass suitable for a detailed mineralogical and chemical study of the process of serpentinization. It is one of several ultramafic masses found in the Franciscan Formation of Jurassic and Cretaceous age that compose the southern part of the Santa Lucia Range. Previous authors have discussed the regional setting, the lithologies within the Franciscan and younger rocks, the age of the body, and the geologic structure. Among these studies are those conducted by WHITNEY (1865), FAIRBANKS (1894), HILL (1923), BELL (1939), and BURCH (1965).

* Publication authorized by the Director, U. S. Geological Survey.

The present study was begun at the University of California, where much of the work was done. Research has been continued by the author as an employee of the U. S. Geological Survey.

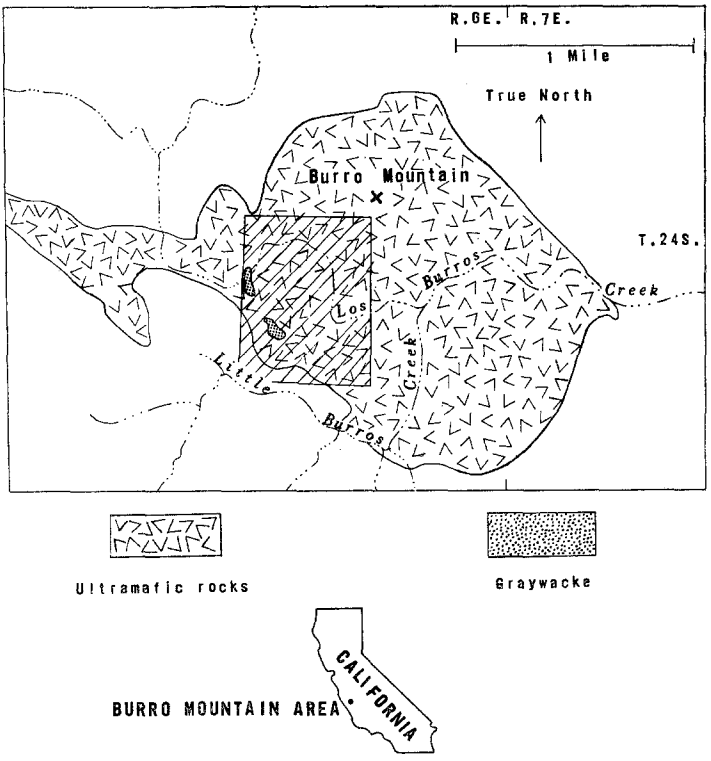

Fig. 1. Location and sketch map of the Burro Mountain area. Hachured area is shown in Figs. 3 and 4

General Geology

The ultramafic complex is 1 to $1^1/_2$ miles in diameter and consists of partially or wholly serpentinized peridotites and dunites. The peridotite ranges from a homogeneous olivine-pyroxene rock alternating with layers of dunite, through a rock with disturbed layers apparently due to fine fracturing that yields a mottled texture, to a rock which is not layered.

The dunites comprise at least three general structural types, including: (1) Dunite layers, 0.5 inch to tens of feet thick, that generally trend north-south and have a subvertical dip. (2) Large dunite bodies with an outcrop pattern several thousands of feet long and 350 to 500 feet in maximum width. These are generally concordant with the finer scale dunite layering but in detail are discordant. (3) Small, very irregular and discordant crosscutting dunite masses and dikes that appear to be later than the other two structural types and the peridotite and show crosscutting relations with all other rock types.

Besides the primary rocks, serpentinites are present and can be divided into two groups, blocky or massive and sheared. Blocky serpentinites are those broken by joints and faults with little or no displacement into blocks which range in size from 2 cubic feet to 50 or more cubic feet. Although partially or completely serpentini-

zed, they preserve and consistently retain the textures of the parent rock. Cross-fiber and slip-fiber asbestos fill numerous fractures, but rarely do the veins filling the fractures develop to a width of more than 1 inch.

Sheared or slickensided serpentinite is found within the shear and fracture zones of the ultramafic mass. It lines most of the faults and joints within the main mass but is most abundant near the margins. In a few places, the sheared serpentinite contains large blocks of coherent massive rock in which the texture of the parent material is preserved, but generally this texture is obliterated.

Structures within the ultramafic mass include a fracture cleavage that is defined both in the field and in thin section by a fine fracturing in the peridotite and locally in the dunite. It strikes northeast and dips either vertically or steeply to the southeast or northwest. A second, less pervasive kind of fracture cleavage is locally developed parallel to faults cutting the ultramafic body and dies out rapidly away from the fault planes. Veins of serpentine tend to parallel the cleavages as well as occupy their older fractures.

In addition to these cleavages, most of the olivine in the peridotite and dunite is broken up into cubical blocks. The exception to this is fine-grained olivine which forms mosaiclike textures. This cubical fracture with minute or no offset is ubiquitous throughout the olivine in the ultramafic mass.

There are several sets of faults, including border faults, both low angle and high angle, to which the degree of serpentinization appears to be spatially related. All the larger sheared serpentine masses are localized along and within the fault zones.

Petrology of the Primary Ultramafic Rocks

Dunite. — Primary minerals in the Butto Mountain dunites are olivine, enstatite, spinels, and occasionally diopside. Alteration of this rock yields chrysotile, lizardite, brucite, talc, magnetite, and magnesite. Opaque phases identified include awaruite, heazlewoodite, pentlandite, and pyrrhotite. The chemical composition is simple, consisting of over 96 percent of MgO, SiO_2, irons oxides, and water, as is shown by chemical analyses given by Burch (1965).

The texture of unaltered dunite is allotriomorphic inequigranular in which olivine grains average 2 to 3 millimeters in diameter but include a large number of grains that have dimensions of 4 by 1 to 5 by 2 mm. Occasionally the large grains enclose several smaller euhedral crystals of olivine that average 0.2 to 0.4 mm in diameter. In outcrop, olivine individuals were observed which attained sizes of several centimeters. Enstatite individuals in the dunite rarely attain diameters greater than 2 to 3 mm. All dunites observed in thin section showed olivine (excluding mosaiclike olivine) that was broken up by fractures into squares, rectangles, and occassionally irregular fragments less than a half a millimeter in diameter. Further descriptive material, including modes, is given by Page (1966).

Peridotite. — The primary mineralogy of the peridotites consists of olivine, enstatite, diopside, and spinel and is very similar to that of the dunite except for a greater abundance of pyroxenes. Upon alteration, the number of minerals present is increased by the appearance of lizardite, chrysotile, brucite, talc, magnetite, actinolitic amphibole, and, locally, carbonates. The following opaque minerals are identified in polished specimens and on the electron probe: awaruite, heazlewoodite, pentlandite, and pyrrhotite. Chemical analyses of the peridotite are given by Burch (1965).

The peridotites have an interlocking granular texture composed of olivine and enstatite grains that average 1 to 2 mm in diameter but include a few individual olivine grains attaining sizes of 3 or more mm. In general, the grain size of the peridotite is smaller than that of the dunite. As was observed in the dunite, olivine in the peridotites is finely fractured in thin section into squares and rectangles less than 0.5 mm in length; in a few samples the enstatites are fractured on the same scale. In thin section, olivine is in contact with enstatite, diopside, and chromite

as well as with the alteration products. Other features of olivines observed in thin section in both peridotites and dunites include: (1) widespread undulatory extinction in the larger crystals, (2) fluid and spinel inclusions planes, (3) deformation lamellae parallel to the (100) plane (BURCH, 1965), (4) mortar texture that consists of fine-grained olivine mosaic, and (5) fine fracturing parallel to three perpendicular planes. Undulatory extinction was not observed in the fine grained olivines which form the mosaic texture around the larger grains. Further descriptive material, including modes, is given by PAGE (1966).

Mineralogy of the Dunite and Peridotite

Olivine. — Analyses of olivine made with the electron-probe microanalyzer indicate a range of $Fo_{90.8}$ to $Fo_{91.6}$. In table 1 are microprobe analyses and calculated formulae of olivines from both dunite and peridotite made for SiO_2, Al_2O_3, FeO[1], and MgO. Olivine analyses consisting of ten or more beam spots per grain and five to ten grains per sample for MgO, FeO, and SiO_2 are plotted as averages in Fig. 2. Probe traverses across individual olivine grains show that all olivine grains in individual hand specimens are remarkably uniform in composition. Olivine compositions throughout the body, wheter in dunite or peridotite, vary in FeO by less than 1 weight percent. Optical and X-ray determinations support this small compositional variation (BURCH, 1965; PAGE, 1966).

Enstatite. — Orthopyroxene ($2V_z=57—91°$) occurs in relatively small amounts and has exsolution lamellae of diopside parallel to (100). Enstatite was observed in contact with olivine, spinel, diopside, and those minerals produced by alteration. Locally, bent crystals of enstatite were observed.

Table 1 presents microprobe analyses of enstatites and calculated formulae, and Fig. 2 gives average partial enstatite analyses for widely spaced samples. As seen from Fig. 2, the MgO to FeO ratio is practically invariable throughout the ultramafic mass, but table 1 shows that SiO_2, Al_2O_3, and CaO content of enstatites does vary slightly. The $Mg^{+2}/[Mg^{+2}+Fe^{+2}+Al^{+3}(IV)]$ ratio of enstatites varies from $En_{85.8}$ to $En_{90.2}$.

Clinoppyroxene. — In the dunites, clinopyroxene ($2V_z=52—64°$, $Z\lambda c=30—42°$) occurs only as lamellae in enstatite, whereas in the peridotites, it also occurs as independent grains and as fillings in crosscutting fractures in enstatite. The clinopyroxene in the fractures appears to be continuous with the clinopyroxene of the lamellae. Optical properties indicate that the mineral is diopside. Since clinopyroxenes are extremely sparse and difficult to identify in the optical system of the electron microprobe, only one total analysis was made (Table 1). Partial analyses of clinopyroxenes indicate approximately the same composition as given in table 1 (from PAGE, 1966).

Spinel. — The only spinel, besides magnetite, occurring in both the dunite and the peridotite, is a reddish-brown translucent mineral in transmitted light. It is commonly idiomorphic in the dunite, especially where it forms layers. Elsewhere, spinel occurs filling interstitial spaces in the olivine framework clots and lenses, suggesting that it was a late phase to crystallize. It is a chromian spinal or, more aptly, picotite according to BURCH (1965), who presents its chemical and physical properties.

[1] In all microprobe analyses discussed, the oxidation state of iron can not be distinguished and therefore all analyses report total iron as FeO. Microprobe techniques used are discussed by PAGE (1966).

Table 1. *Electron microprobe analyses and calculated formulae of olivines, enstatites, and diopside from the Burro Mountain ultramafic complex. Experimental conditions on an ARL Microanalyzer; 15 kv excitation potential, 0.06 microamps sample current, 20 seconds integration time, and probe spot ca. 0.5 microns in diameter. Minerals used for standardization discussed by* PAGE *(1966)*

Oxide	Olivines								Enstatites							Diopside
	1	2	3	4	5	6	7	8	9	10	11	12	13	14	15	16
SiO_2	41.0	40.9	40.7	40,7	40,7	40.8	40.9	40.5	56.7	56.8	54.4	56.3	57.7	56.3	54.8	51.1
Al_2O_3	0.0	0.0	0.0	0.0	0.0	0.0	0.0	0.0	2.8	1.8	3.9	1.5	1.4	3.2	2.6	3.4
FeO*	8.9	8.8	8.7	8.6	8.2	8.7	8.2	8.7	6.0	5.5	5.7	5.4	5.3	5.7	5.6	1.8
MgO	49.3	50.4	49.8	49.8	50.2	49.7	50.7	50.6	33.0	34.9	35.1	35.0	34.9	34.5	35.5	17.9
CaO	~0.04	~0.01	~0.06	~0.04	~0.04	~0.04	~0.04	~0.01	0.9	0.6	0.6	0.9	1.1	0.8	0.7	25.9
Total	99.2	100.1	99.3	99.1	99.1	99.2	99.8	99.8	99.4	99.6	99.7	99.1	100.4	100.5	99.2	100.1
Ion	*Formulae based on 4 (0)*								*Formulae based on 6 (0)*							
Si^{+4}	1.006	0.996	0.999	1.000	0.998	1.001	0.996	0.990	1.961	1.958	1.882	1.954	1.973	1.927	1.906	1.868
Al^{+3}	—	—	—	—	—	—	—	—	0.039	0.042	0.118	0.046	0.027	0.073	0.094	0.132
Sum Tetrahedral	1.006	0.996	1.999	1.000	0.998	1.001	0.996	0.990	2.000	2.000	2.000	2.000	2.000	2.000	2.00	2.00
Al^{+3}	—	—	—	—	—	—	—	—	0.075	0.031	0.041	0.015	0.029	0.056	0.012	0.014
Mg^{+2}	1.804	1.829	1.822	1.823	1.834	1.818	1.840	1.843	1.701	1.793	1.810	1.810	1.778	1.760	1.840	0.975
Fe^{+2}	0.183	0.179	0.179	0.177	0.168	0.179	0.167	0.178	0.174	0.159	0.165	0.157	0.152	0.163	0.163	0.055
Ca^{+2}	0.001	0.0003	0.002	0.001	0.001	0.001	0.001	0.0003	0.033	0.022	0.022	0.034	0.040	0.029	0.026	1.014
Sum Octahedral	1.988	2.008	2.002	2.001	2.003	1.997	2.008	2.021	1.907	1.973	1.997	2.001	1.969	1.950	2.029	2.059
$\frac{Mg^{+2}}{Mg^{+2}+Fe^{+2}+Ca^{+2}}$	90.8	91.1	91.0	91.1	91.6	91.0	91.6	91.2	$\frac{Mg^{+2}}{Mg^{+2}+Fe^{+2}+Ca^{+2}+Al^{+3}\,(IV)}$ 85.8	89.4	88.8	89.8	89.0	87.6	90.2	47.4

1 = 8133 AX, olivine in peridotite in joint blocks
2 = 8241 Fb, olivine in peridotite
3 = 8241 Gb, olivine in dunite
4 = 8284 Gb, olivine in dunite band
5 = 8305 B, olivine in peridotite dike which intersects dunite band
6 = 9142 By, olivine in peridotite band
7 = 9161 By, olivine in dunite band
8 = 8245 y, olivine in serpentinized peridotite
9 = 8133 AX, enstatite, same as 1
10 = 8176 X, enstatite in peridotite
11 = 8241 Fb, enstatite in peridotite
12 = 8284 Gb, enstatite, same as 4
13 = 8305 B, enstatite, same as 5
14 = 9142 By, enstatite, same as 6
15 = 9245 y, enstatite, same as 8
16 = 9245 y, diopside, same as 8 and 15

Sample numbers are those of S. H. BURCH of the U.S. Geological Survey, Menlo Park, Calif., locations are given in BURCH (1965).
* FeO is total iron.

Petrology of the Serpentinites

The density of both olivine of composition $Fo_{90}Fa_{10}$ and enstatite of composition $En_{90}Fs_{10}$ is approximately 3.30 g/cc, and the density of serpentine is about 2.50 g/cc; therefore, the density of the dunite and peridotite reflects the degree of serpentinization. A density of 3.10 g/cc indicates that the rock is approximately

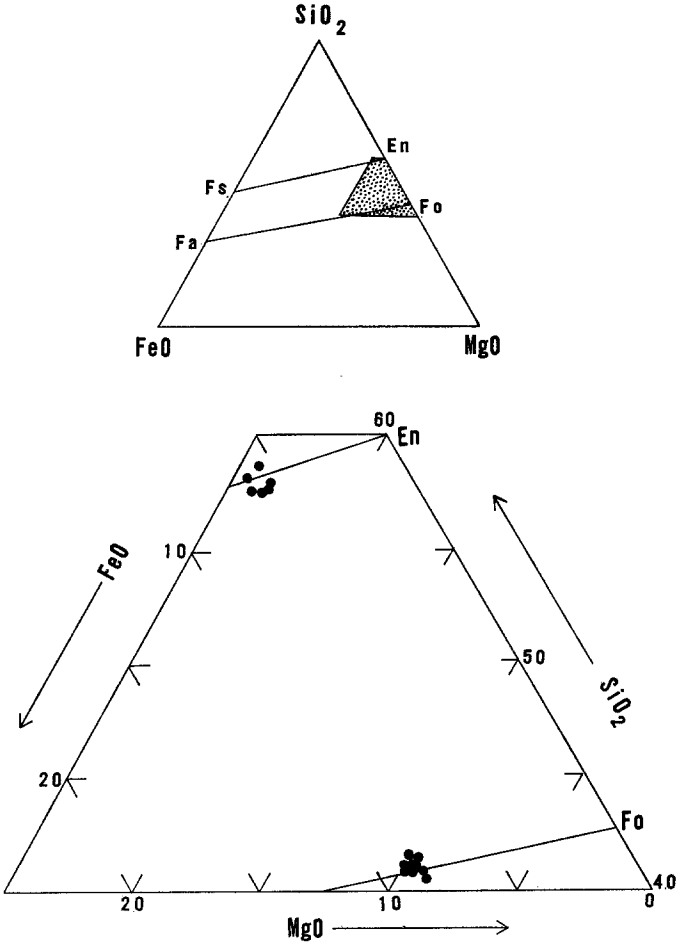

Fig. 2. Average microprobe analyses of olivine and enstatite from Burro Mountain plotted an a triangular diagram of MgO-FeO (total iron)-SiO_2 weight percent. Lower diagram from stippled area in upper triangle

25 percent serpentinized; 2.90 g/cc, 50 percent; and 2.70 g/cc, 75 percent. Although density is by no means an exact measure of serpentinization, since chromite and clinopyroxenes are present in the parent material, and magnetite, talc, and brucite in the serpentinized rock, it is an excellent guide to the gross pattern of alteration. BURCH (1965) measured the density of 471 cores from the Burro Mountain ultramafic mass and correlated the degree of serpentinization in relation to data on remnant magnetization. The cores were taken on an east-west traverse through the body. Unfortunately, he did not have a detailed geologic map with which to compare the density data, but he was able to draw the conclusions (1) that the

median density is 2.93 g/cc and the extremes 2.30/g cc and 3.30 g/cc; (2) that the densities appear to decrease outward toward the margins, although there are zones of lighter density within the body; and (3) that at the eastern margin the density change is gradual, whereas at the western margin it is quite sharp.

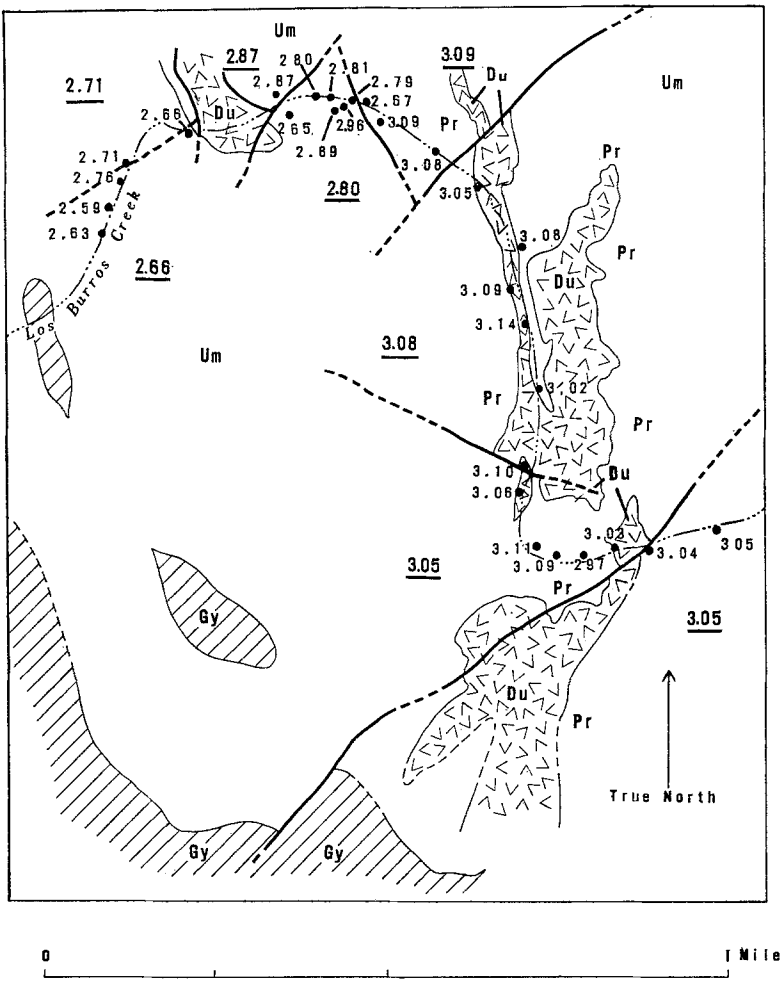

Fig. 3. Density (g/cc) of peridotites compared with detailed geology of the southeastern part of the Burro Mountain mass along Los Burros Creek. See Fig. 1 for location. *gy* graywacke; *um* undifferentiated ultramafic rocks; *du* dunite; *pr* peridotite; thin lines, contacts; heavy lines, faults; dots and numbers, density; underlined numbers, average density for fault block

Part of Burch's density data are plotted on a section of a detailed geologic map of 1:6000[2] for a section of Los Burros Creek located near the eastern margin of the main ultramafic mass (Figs. 3 and 4). Each given density at a located point represents either the value for an individual core or an average of cores taken at that location. The geologic and density data of Figs. 3 and 4 indicate that although serpentinization increases toward the margin, the actual distribution may

[2] The geologic map was prepared by N. Page and R. Loney in 1965.

be more closely controlled in space by faults and shear zones at the margins and within the main mass. A study of density data taken from Little Burros Creek, a north-south trending stream that crosses the contact, indicates that on the southern margin of the body, serpentinization is more regular, with a sharp exponential increase towards the margin (PAGE, 1966).

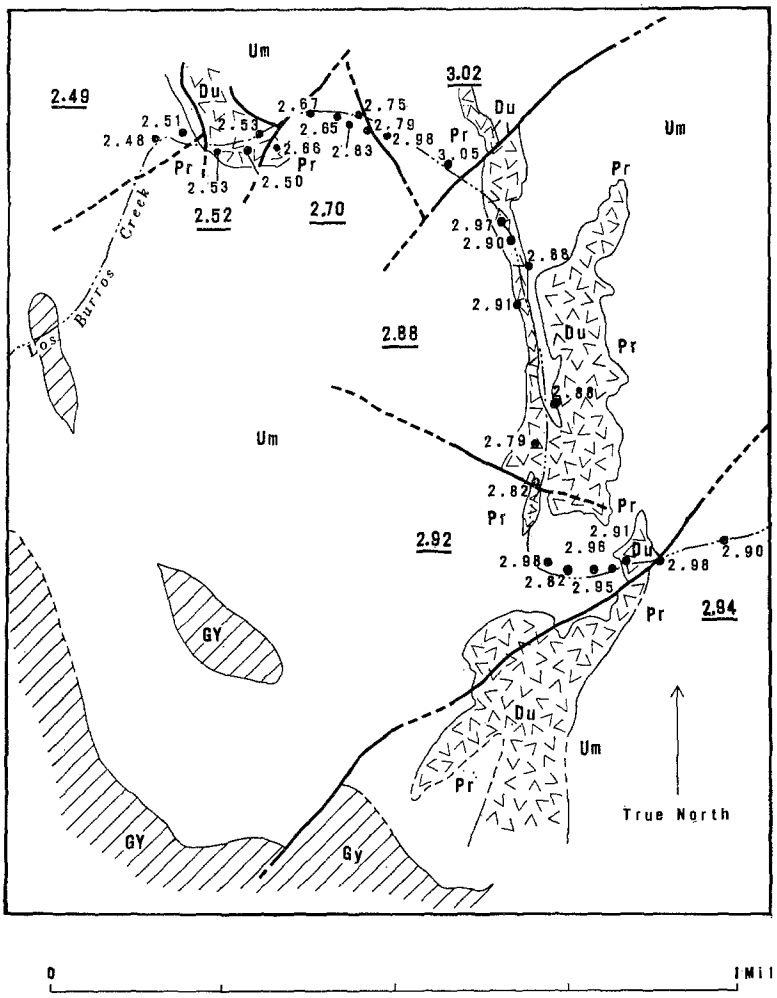

Fig. 4. Density of dunite compared with detailed geology of a southeastern part of the Burro Mountain mass. See Fig. 1 for location; symbols are the same as in Fig. 3

Three main textural types of serpentine occur at Burro Mountain, and all textures observed are composed of one or more of these types, which are: (1) colorless to pale green lizardite pseudomorphs after enstatite (bastite); (2) dark-green, irregular, platy serpentine combined with areas of cross and slip-fiber serpentine replacing olivine (mesh structure); and (3) late crosscutting colorless, cross-fiber chrysotile (veins). Type (2) when X-rayed is found to be composed of lizardite and chrysotile in which one or the other may be dominant in any one sample. Asso-

ciated with types (2) and (3) may be brucite or magnetite, or both. The three main groups have occasionally undergone tectonic processes which change their textures into at least two different kinds: one is designated the "ribbon or band" structure; the other is simply sheared serpentinite.

The textural development of the serpentinites is described in density groups which represent the different degrees of serpentinization. Dunites and peridotites with densities between 3.30 and 2.95 g/cc exhibit the same alteration pattern. In the densest rock, the three perpendicular fracture sets are visible, but in the interlocking olivine and enstatite grains generally, they are tight and do not contain serpentine. The first development of serpentine is concurrent with open partings, allowing avenues for the penetration of water, in which the olivine and the enstatite are usually granulated. This finer grained material is altered to greenish serpentine which occurs in the form of irregular plates and masses. Brucite does not develop at this stage nor is much magnetite formed. As the degree of serpentinization increases, serpentine continues to form at the expense of olivine and enstatite in the three fracture sets. The serpentine formation as described thus far is pervasive throughout the entire ultramafic mass. As alteration proceeds, brucite plus serpentine is formed from olivine, and in the rocks where pyroxene is present, lizardite forms along the mineral cleavages at the end of the grains. In these stages, the spinel remains unaffected and large amounts of magnetite are formed.

Differences between the alteration of dunite and peridotite begin to appear in rocks of density between 2.95 and 2.75 g/cc. In the dunite, individual fragments of fractured olivine grains are now separated by wide areas of cross and slip-fiber serpentine which occurs in irregular masses and platelets with brucite. Brucite tends to rim most of the olivine fragments, separating the serpentine from the olivine. In peridotites, a dark-green serpentine is observed to replace the olivines; but the remnant enstatites are located in bastites of colorless lizardite. In all rocks, the framework is developed which will form the mesh structure. More magnetite is formed in this stage and the spinels begin to have margins and veins of magnetite. Serpentinites with densities of 2.75 and 2.50 g/cc have the well known mesh and bastite structures with remnant olivine and pyroxene. Generally, both of these textures may be cut by late clinochrysotile veins which generally parallel the northeast-trending pervasive cleavage and locally follow the cleavages which parallel the numerous faults. Magnetite is very abundant. As chrysotile veinlets develop, more magnetite forms and concentrates within the clearer, transparent veins and gashes. When tectonic processes rearrange the textures, magnetite develops an euhedral habit and becomes predominantly associated with veins. In mesh centers, brucite occurs intimately associated with the serpentine. Locally, brucite veins are developed which cross-cut the serpentine meshes.

Mineralogy of the Alteration Products

A detailed mineralogic study of the serpentines, brucite, and other alteration products of dunites and peridotites should yield limiting information for conjectures and interpretation concerning the serpentinization process. Fifty-three core samples were studied in detail. All samples were ground to less than 100 mesh but greater than 325 mesh. The light separate (liquid density 2.80 g/cc) of a bromoform separation was X-rayed on a diffractometer and the identification of serpentine minerals was based on the scheme of WHITTAKER and ZUSSMAN

(1956). Both the light separates and grains picked from the uncrushed rock samples were used to establish the alteration mineralogy. Other samples were studied by similar methods in combination with thin sections and microprobe analyses.

Serpentines. — All X-ray identifications of serpentine yielded only lizardite and chrysotile. No antigorite was identified. An estimate of relative amounts of the two minerals is based on relative peak heights or intensities of the (202) reflection of lizardite and the (202) reflection of chrysotile; this is unsatisfactory as a quantitative technique because of the large changes in intensity caused by sample orientation. Yet, using the same sample preparation technique for each sample, studied, a qualitative estimate is of some value. From the results where olivine and pyroxene were eliminated in the bromoform separations and the two mineral species could be identified, the amount of lizardite in 80 percent of the samples is either greater than or equal to the amount of chrysotile. In 70 percent of the peridotites and in 90 percent of the dunites, lizardite is the main serpentine. The relative abundance of the serpentine minerals is not related to the degree of serpentinization nor, apparently, to the location of the sample with respect to the margins of the body. X-ray patterns of individual bastites drilled from peridotites and separated from the pyroxene indicate that the bastites are lizardite with no chrysotile added.

The ranges in serpentine d-spacings, measured on X-ray patterns against a silicon internal standard, are: for the (202) d-spacing of lizardite, 2.49 to 2.52 Å, and for the (202) d-spacing of chrysotile, 2.43 to 2.46 Å. These variations could not be correlated with either rock type or degree of serpentinization, since in most samples they represent average lizardite or chrysotile compositions.

Compositional variations of serpentine minerals and mixtures were obstained by using the electron microprobe analyzer on selected polished thin sections, which avoided the problems inherent in separation of fine grained intimate mixtures for wet chemical analyses. Microprobe analyses can be directly related to petrological details, since a correlation of the X-ray work with observations in thin sections makes it possible to identify, by texture and optical character, the serpentine mineral or mixture of minerals. One problem which interfers with direct analysis of each grain of serpentine or brucite is that magnetite, serpentine, and brucite are intergrown on a fine scale. A probe traverse across such an intergrowth at 5- to 10-micron intervals between individual spots yields a series of bulk rock analyses for Mg, Fe, and Si. Those that fall on brucite only lack Si, and those that fall on magnetite only lack Mg and Si. In actuality, only magnetite occurs in distinct and large enough individuals to show no Mg and Si. Also, magnetite is very easy to identify optically in reflected light under the microprobe. When brucite and serpentine occur in a mixture, assuming that the brucite and serpentine to the first approximation have a constant composition in each individual crystal or grain, it is possible to indirectly derive the composition of the serpentine and the brucite. All microprobe analyses on the traverse are bulk analyses of a particular pair of brucite and serpentine, and should fall on a single tie line, and for the pairs analysed they do.

Lizardite occurring in bastites represents the most iron-rich serpentine in a rock. Fig. 5 a—i shows lizardite (bastites) compositions for individual rocks; Fig. 6 A gives a composite of all lizardite compositions in serpentinites from Burro Mountain. In Fig. 6 A, the composite field is split up into the density groups of 3.30 to 2.95 g/cc, 2.94 to 2.75 g/cc, and 2.74 to 2.50 g/cc. In general, high-density rocks correspond with the central part of the ultramafic and lowest density rocks with the margins of the ultramafic mass. Lizardites from the margin exhibit greater FeO-MgO variation than those from the core. Individual lizardites from the margin have the largest amount of FeO, as well as the largest amount of MgO. Those from the core exhibit smaller variation and are not enriched in total iron.

Although chrysotile occurs in veins, analyses of chrysotile occurring by itself are rare because brucite also occurs in the veins. Analyses as plotted on Fig. 6 B show lower iron content for chrysotile than for lizardite. No trend of composition with density is observed.

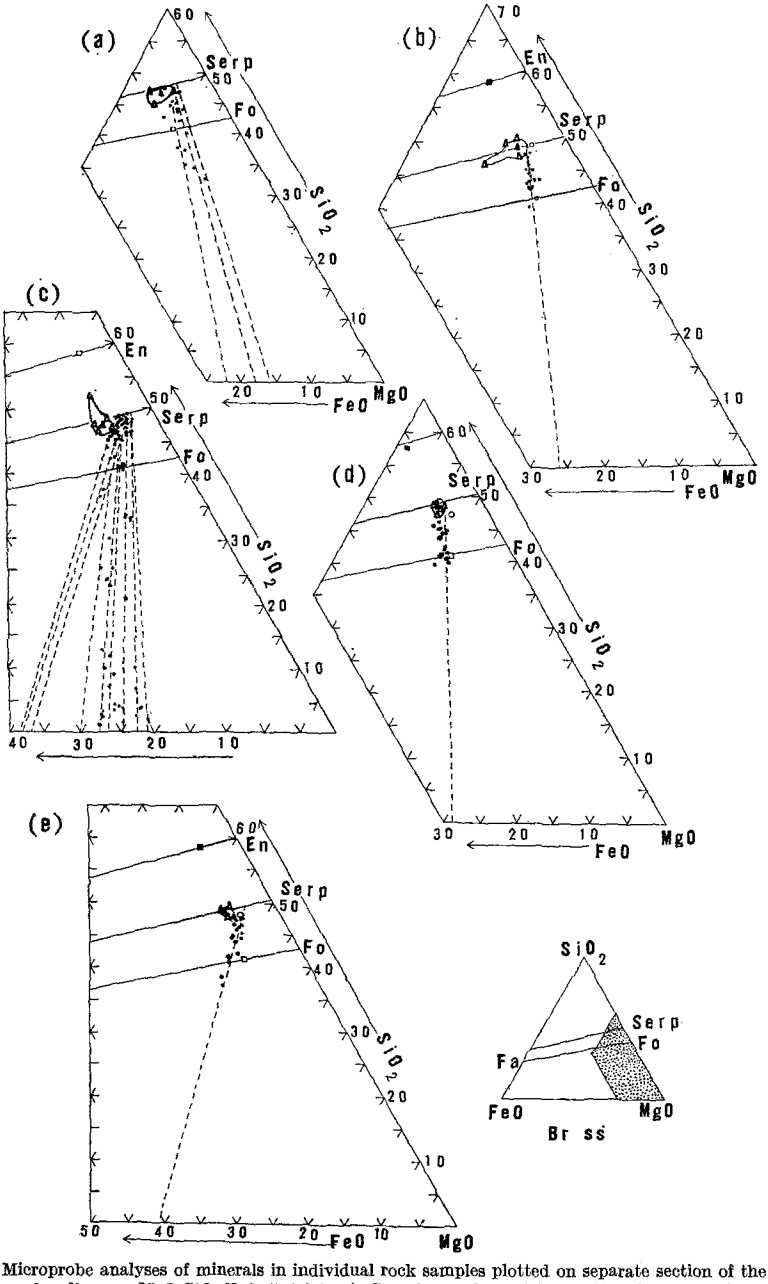

Fig. 5a—i. Microprobe analyses of minerals in individual rock samples plotted on separate section of the weight percent triangular diagram MgO-SiO_2-FeO (total iron). Sample numbers: (a) 9245 Y, (b) 8176 X, (c) 8284 Gb, (d) 8207 t, (e) 8305 B, (f) 9161 By, (g) 9142 By, (h) 8241 kc, (i) 9226 cx. Sample locations given by BURCH (1965)

Since most of the analyses obtainable from a probe specimen are of mixtures of lizardite, chrysotile, and frequently brucite, all limiting tie lines between brucite and serpentine (mesh structures) are collected from Fig. 5 (a—i) and put on the triangular diagram, Fig. 7. The tie line (3a of Fig. 7) which connects iron-rich

brucite and magnesium-poor serpentine appears to be anomalous but represents conditions under which large amounts of magnetite formed. All analyses which established this tie line were from late chrysotile and lizardite veins in which magnetite is abundant. Except for this, high-density rocks (core rocks) have the

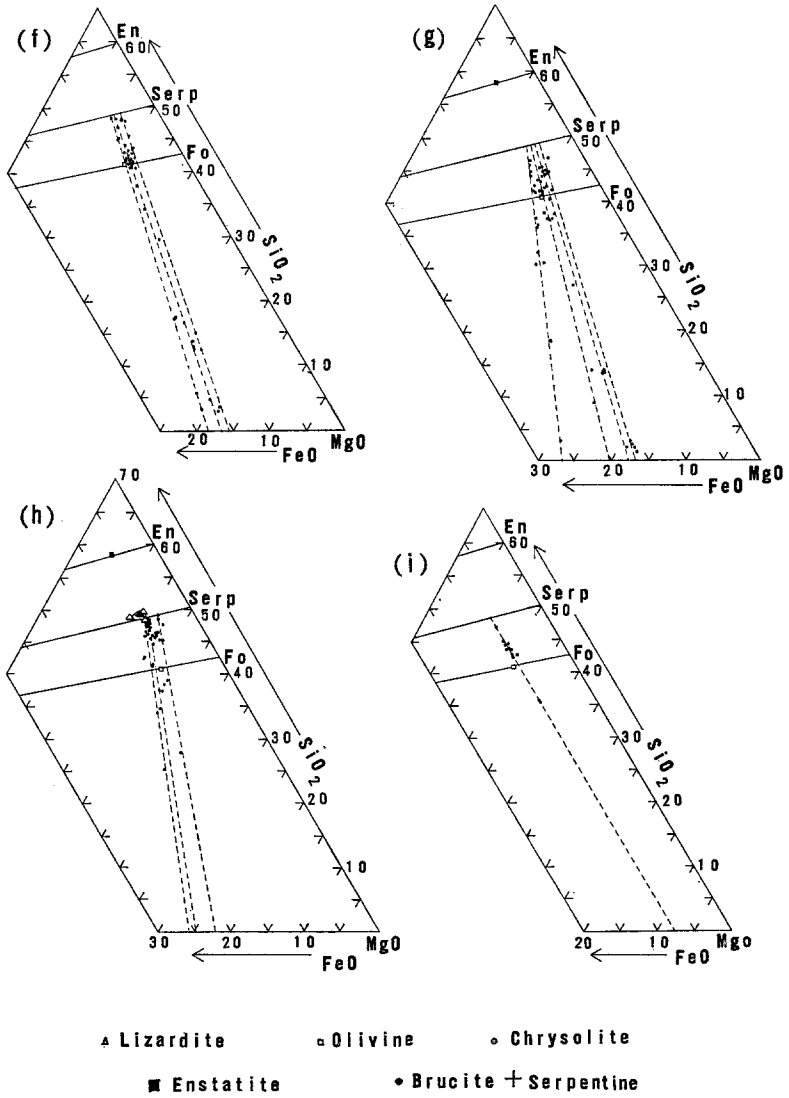

Fig. 5 f—i (for legend see p. 331)

broadest range of variation in composition of brucite and the most magnesium-rich brucites. Margin rocks (low-density) have the most iron-rich brucite and a smaller range of variation. Serpentine mixtures of chrysotile and lizardite (mesh structure) from the core (tie lines 1 and 2) are more iron-rich and have a narrower

range in composition than serpentine mixtures from intermediate density rocks (tie line 3 and 4). Serpentine mixtures of marginal rocks (tie lines 5 and 6) show the broadest range of composition and include the most magnesium-rich serpentine. Parent rock type, dunite or peridotite, has no apparent effect on the serpentine compositions. The main geological variables are the degree of serpentinization, relation to the margin of the body and faults and shear zones, and possibly time of formation.

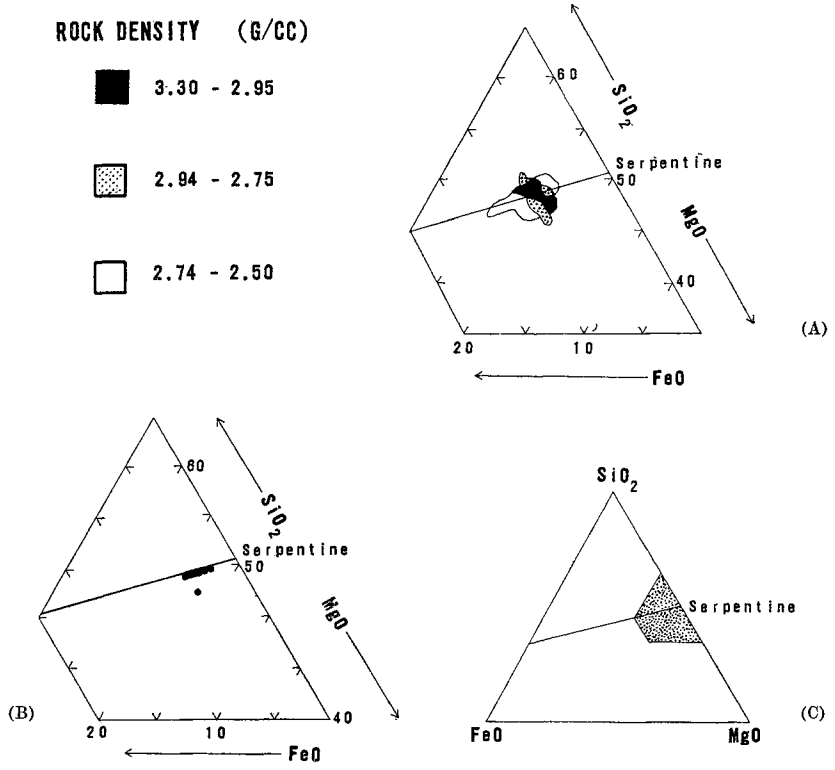

Fig. 6 A—C. Serpentine microprobe compositions given in MgO-SiO_2-FeO (total iron) weight percent. (A) bastites divided into rock density groups; (B) chrysotiles; (C) reference triangle

Brucite. — HOSTETLER and others (1966) demonstrate that the brucite from ultramafic masses of the circum-Pacific mountain belt contain from 5 to 25 mol percent $Fe(OH)_2$. At Burro Mountain the variation in brucite compositions is correlated with location of the sample in the mass, association of parent and alteration minerals, and position in textural development.

In dunites and peridotites of the 53 core samples, brucite, as mentioned above, occurs as rims around olivines which are not completely serpentinized and intermixed with serpentine as central cores of meshes. Locally, brucite occurs as isolated, late-formed veins that contain traces of serpentine and in chrysotile veins. A correlation between the amount of brucite present and rock type is shown by using the intensity ratio of the (001) reflection of brucite to the (004) reflection of

serpentine plus (001) brucite from X-ray diffraction patterns. On the average, the intensity ratio for dunites indicates about twice the amount of brucite as is contained in peridotites (Fig. 8a). Correlation of rock density and rock type with the brucite-serpentine intensity ratio (Fig. 8b) demonstrates that as density decreases, the proportion of brucite to serpentine increases. Dunites tend to have larger amounts of brucite than peridotites with the same density.

As measured by the microprobe, the composition of brucite ranges in FeO from 16 to 43 weight percent. Further information on the variation in brucite composi-

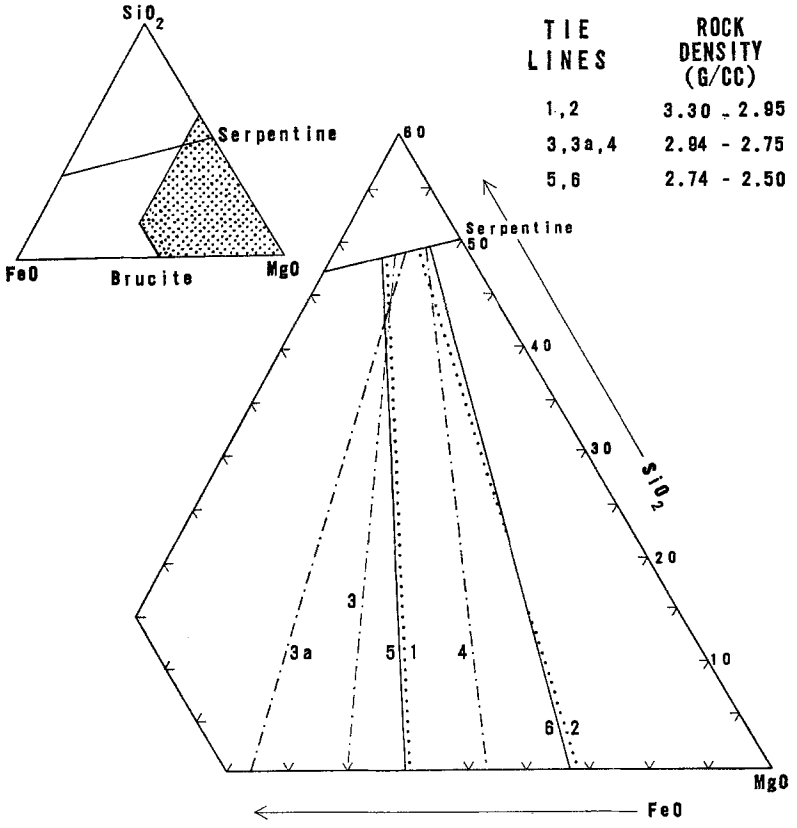

Fig. 7. Limiting tie lines for brucite serpentine pairs for rock density groups abstracted from Fig. 5. Lower diagram from stippled area in upper triangle

tion comes from the $d_{(001)}$ brucite, measured for 51 samples and found to vary between 4.77 Å and 4.68 Å. The majority of the brucites have $_{(001)}$ of 4.72 to 4.74 Å. The $d_{(001)}$ of pure brucite is 4.77 Å and the $d_{(001)}$ of $Fe(OH)_2$ is 4.597 Å. Assuming a linear relationship between mol percent $Fe(OH)_2$ and $d_{(001)}$ would indicate limits of substitution of 0 to 50 mol percent $Fe(OH)_2$, with the majority of the brucites having between 18 and 32 mol percent $Fe(OH)_2$. No correlation of brucite compositions with rock type was discerned, but composition is related to the density and hence its position within the ultramafic body.

Amphibole. — A colorless amphibole (negative 2 V, $X\lambda c = 20—21°$, termolite-actinolite) was observed in small amounts in a few thin sections from samples near the center of the body. It is mixed with talc, and locally with serpentine, and

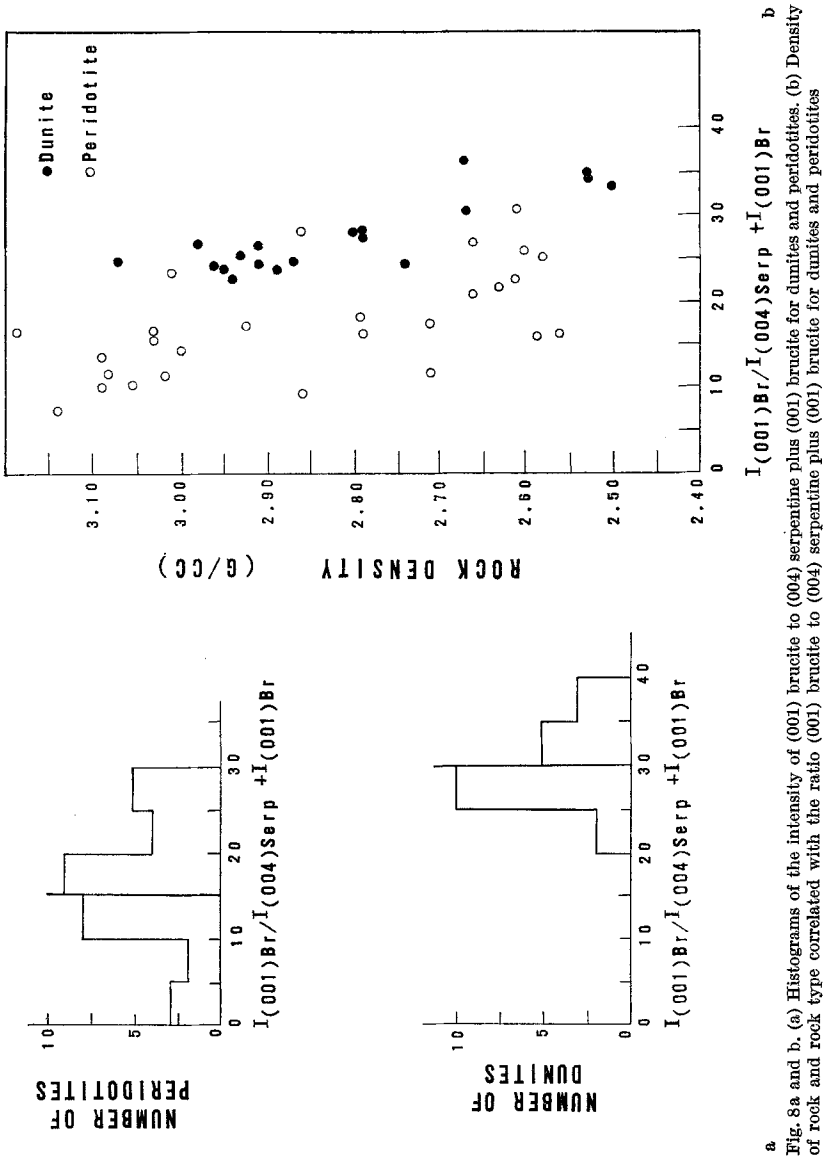

Fig. 8a and b. (a) Histograms of the intensity of (001) brucite to (004) serpentine plus (001) brucite for dunites and peridottites. (b) Density of rock and rock type correlated with the ratio (001) brucite to (004) serpentine plus (001) brucite for dunites and peridotites

occupies a position which previously was apparently occupied by enstatite and diopside.

Talc. — Two types of occurrences were observed for talc. One in which fine-grained talc, mixed with carbonate, forms late veins which cross-cut all other phases in

the rock and one in which talc appears to pseudomorph enstatite. Olivine of the original rock appears unaffected.

Magnetite. — In addition to primary magnetite, secondary magnetite seems to be derived from at least three different alteration processes. The primary spinel, picotite, alters on its margins and in fractures to magnetite; this becomes important toward the end of serpentinization. Also late in serpentinization, both olivines altering to serpentines and previously formed serpentines appear to lose iron, which goes into magnetite. Some vein serpentines also appear to be partially recrystallized, and in the process react to form new serpentine plus magnetite. Apparently very little of the magnetite is formed in the early stages of serpentinization; rather, as the degree of serpentinization increases, the amount of magnetite increases. In support of this, BURCH (1965) found that the magnetic susceptibility of the rock increases with decreasing density.

Other ore Minerals. — Awaruite, pentlandite, heazlewoodite, and pyrrhotite were identified qualitatively with the electron microprobe and in polished specimens. The time and space relations of these minerals with the primary and alteration phases is undetermined, but they were probably formed during the process of serpentinization.

Discussion

Petrogenesis of the Primary Ultramafic Complex

The sheared margins of serpentinite, abundance of small displacement faults, development of fine fractures, and absence of high-temperature contact rocks indicate that the ultramafic complex at Burro Mountain attained its present position in the crust by tectonic processes. The presence of the primary minerals olivine, enstatite, diopside, and spinel suggest that the body was, at some time and position, hot, at least hot enough to form minerals which are homogenous in composition and with the ubiquitous interlocking granular texture. This stage certainly was finished before the initial formation of serpentine.

Within the Burro Mountain mass are textures suggestive of deformation and later recrystallization. These are: (1) bent enstatite crystals, (2) mortar or mosaic textured olivine, (3) large olivine individuals in the dunite, (4) exsolution lamellae in the pyroxenes, and (5) the fine ubiquitous fractures in the olivines. This more or less implies a tectonic event subsequent to emplacement.

Petrogenesis of the Altered Ultramafic Rocks

During the cooling history of the ultramafic complex, probably prior to the commencement of serpentinization, enstatite and clinopyroxene reacted with water to form talc and tremolite. For such a reaction to proceed, either SiO_2 must be added to the reactants, or excess MgO is produced. At Burro Mountain, this reaction does not involve large amounts of material, as is evidenced by the local nature of talc-tremolite pseudomorphs and intermixed serpentine. BOYD's experimental work (1954, 1959) on the breakdown of tremolite to enstatite, diopside, quartz, and water sets an upper temperature limit of 840° to 880° C. If the upper stability limit of talc were well known, then this would constitute the upper limit for the above coupled reaction. BOWEN and TUTTLE (1949) reversed the reaction of talc = enstatite, quartz, and water, but evidence present by FYFE (1962) on the reactions

talc = anthophyllite, quartz, and water and the higher temperature reaction anthophyllite = enstatite, quartz, and water suggests that BOWEN and TUTTLE's reaction is a metastable one. FYFE's evidence suggests that the upper limit for talc is below 730° C (FYFE, 1962, Table 1, p. 464); but the curve suggesting that tremolite and talc formed below 730°C is by no means established. Enstatite and diopside remain in the peridotites to take part in later reactions because the amount of water present is not sufficient for reaction.

After the formation of the pervasive fracture system, serpentinization began. Based on the mineralogical textures and compositions, the first reaction was of the following type:

Olivine Enstatite Vapor Chrysotile

$$(Mg, Fe)_2SiO_4 + (Mg, Fe)_2Si_2O_6 + H_2O + O_2 = (Mg, Fe^{+2})_6Si_4O_{10}(OH)_8 +$$

Lizardite Magnetite

$$(Mg, Fe^{+3}, Fe^{+2})_6Si_4O_{10}(OH)_0 \text{ with or without } Fe_3O_4. \quad (1)$$

PAGE (1966) has shown that the basic compositional differences between chrysotile and lizardite are in the content and oxidation state of iron; therefore, the formulae for the serpentine minerals are given as above. Somewhat later in the serpentinization process, brucite appears, which suggests the reaction:

Olivine Vapor Brucite Chrysotile

$$(Mg, Fe)_2SiO_4 + H_2O + O_2 = (Mg, Fe)(OH)_2 + (Mg, Fe^{+2})_6Si_4O_{10}(OH)_8 +$$

Lizardite Magnetite

$$(Mg, Fe^{+3}, Fe^{+2})_6Si_4O_{10}(OH)_8 \text{ with or without } Fe_3O_4. \quad (2)$$

Textural and density relations and electron-microprobe analyses of lizardite, chrysotile, and brucite at Burro Mountain show that probably the first phases to form during alteration are magnesium-rich. Later in the serpentinization sequence, the phases become more iron-rich. At a later time, or possibly at a lower temperature, recrystallization and new alteration tends to form magnetite and magnesium-rich brucites and serpentines (especially cross-fiber chrysotile).

Temperature, Pressure, and Compositional Considerations

OLSEN (1963) calculated univariant curves for the following reactions:

Serpentine Magnetite Olivine Talc Vapor

$$21Mg_3Si_2O_5(OH)_4 + 2Fe_3O_4 = 30Mg_{1.8}Fe_{0.2}SiO_4 + 3Mg_3Si_4O_{10}(OH)_2 + 39H_2O + O_2 \quad (3)$$

Serpentine Magnetite Brucite Olivine Vapor

$$15Mg_3Si_2O_5(OH)_4 + 2Fe_3O_4 + 9Mg(OH)_2 = 30Mg_{1.8}Fe_{0.2}SiO_4 + 39H_2O + O_2. \quad (4)$$

The assumptions inherent in OLSEN's calculations are: (1) olivine form an ideal solid solution, that is, $\Delta H_m = 0$[3], (2) no Fe^{+2} in serpentine, brucite, and talc, (3) no Mg^{+2} in magnetite, and (4) the estimated thermodynamic properties for talc and serpentine are correct. These assumptions are not acceptable for the following reasons:

1. There is a crystal-field-stabilization energy term for Fe^{+2} in olivine which leads to a ΔH_m and therefore a nonideal solid solution series (BURNS, 1965; PAGE, 1966).

[3] ΔH_m is defined as the heat of mixing.

2. Analyses of serpentines show that Fe^{+2} and Fe^{+3} are present in serpentines, while analyses of brucite demonstrate the presence of considerable Fe^{+2}.
3. There may be Mg^{+2} in magnetites and Fe^{+2} in talc.
4. PAGE (1966) has shown that the thermodynamic values for talc, which were available at the time OLSEN's paper was written, were in error and that no experimentally determined values for serpentine of any kind were available.

The only reliable experimental work or calculation on serpentinization reactions that exist are those of BOWEN and TUTTLE (1949), extended and confirmed by KITAHARA and others (1966), in the pure MgO-SiO_2-H_2O system. The addition of Al_2O_3 to this system has been investigated by YODER (1952), ROY and ROY (1954, 1955), NELSON and ROY (1958), GILLERY (1959), and SEGNIT (1963). A platy 7 Å-mineral with approximately the composition of serpentine can be synthesized as the result of this work. Since the Al_2O_3 component does not appear to be important at Burro Mountain during serpentinization, it is disregarded in the following discussion.

The temperatures at which reaction (1) takes place are not well established. The curve representing this reaction must lie at a higher temperature than BOWEN and TUTTLE's serpentine=forsterite, talc, and water curve (1949), since forsterite plus talc is more stable than enstatite plus water in the 500° C region at 1 kilobar. The P_{O_2} must have had values approaching the quartz, fayalite, magnetite buffer, since the primary ultramafic assemblage would yield partial pressures of oxygen close to the buffer.

The temperature and pressure limits for reaction (2) for the pure magnesium brucite have been established by BOWEN and TUTTLE (1949) as 365°C at 1 kb. The addition of Fe^{+2} to the brucite stability field can be considered thermodynamically by assuming an ideal solid-solution model ($\Delta H_m = 0$) for $Mg(OH)_2$—$Fe(OH)_2$ solid solutions and calculating the effect of adding x mol percent of $Fe(OH)_2$ to brucite on the stability field of brucite at 1 atmosphere total pressure. For this model the equation is:

$$\underset{(1)}{Mg_xFe_{1-x}(OH)_2} = \underset{(2)}{xMg(OH)_2} + \underset{(3)}{(1-x)FeO} + \underset{(4)}{(1-x)\,H_2O}, \tag{5}$$

where x is the mol fraction of $Mg(OH)_2$ in the solid solution. The change in free energy and entropy are evaluated between x = 1.0 and 0.0 by

$$\Delta G^\circ_{244} = x\Delta G^\circ_2 + (1-x)\Delta G^\circ_3 + (1-x)\Delta G^\circ_4 - \Delta G^\circ_1 \tag{6}$$

$$\Delta S^\circ_{244} = xS^\circ_2 + (1-x)\,S^\circ_3 + (1-x)\,S^\circ_4 - S^\circ_1. \tag{7}$$

Since $(\delta G/\delta T)_p = -S$ or $(\delta \Delta G/\delta T)_p = -\Delta S$, assuming ΔS of the reaction remains constant and integrating,

$$\Delta G^{p=1}_T - \Delta G^\circ_{244} = \Delta S\,(T_2 - T). \tag{8}$$

Using the thermodynamic values given in Table 2 and evaluating at 1 atmosphere pressure for different values of x leads to the T-composition diagram of Fig. 9. This demonstrates that very large amounts of $Mg(OH)_2$ are required to stabilize brucite solid solutions at high temperatures. At higher pressures all temperatures would be raised, but the curve would retain a similar shape. The assumption of ideal solid solution would appear to be poor, since a considerable ΔH_m term might be derived from the crystal-field-stabilization energy of Fe^{+2} in the brucite struc-

Table 2
ΔG°_{298} and S°_{298} values for brucite, water, wustite, ferrous hydroxide, and iron-bearing brucites

Mineral	Formulae	ΔG°_{298} Kcals	S°_{298} Cal/°C/mol	Reference
Brucite	$Mg(OH)_2$	-199.45 ± 0.55	15.09 ± 0.05	1
Water (1)	H_2O (1)	-56.688 ± 0.015	16.715 ± 0.03	1
Wustite	$Fe_{0.953}O$	-58.76 ± 0.5	13.74 ± 0.10	1
Ferrous hydroxide	$Fe(OH)_2$	-115.57	19.0	2
Fe-brucite	$Fe_{0.1}Mg_{0.9}(OH)_2$	-191.3	16.1	3
Fe-brucite	$Fe_{0.2}Mg_{0.8}(OH)_2$	-183.0	16.9	3
Fe-brucite	$Fe_{0.4}Mg_{0.6}(OH)_2$	-166.3	18.0	3
Fe-brucite	$Fe_{0.6}Mg_{0.4}(OH)_2$	-149.8	18.8	3
Fe-brucite	$Fe_{0.8}Mg_{0.2}(OH)_2$	-133.2	19.2	3

1 = Robie (1962); 2 = Latimer (1952) estimated values; 3 = Page (1966) values derived assuming ideal solid solutions.

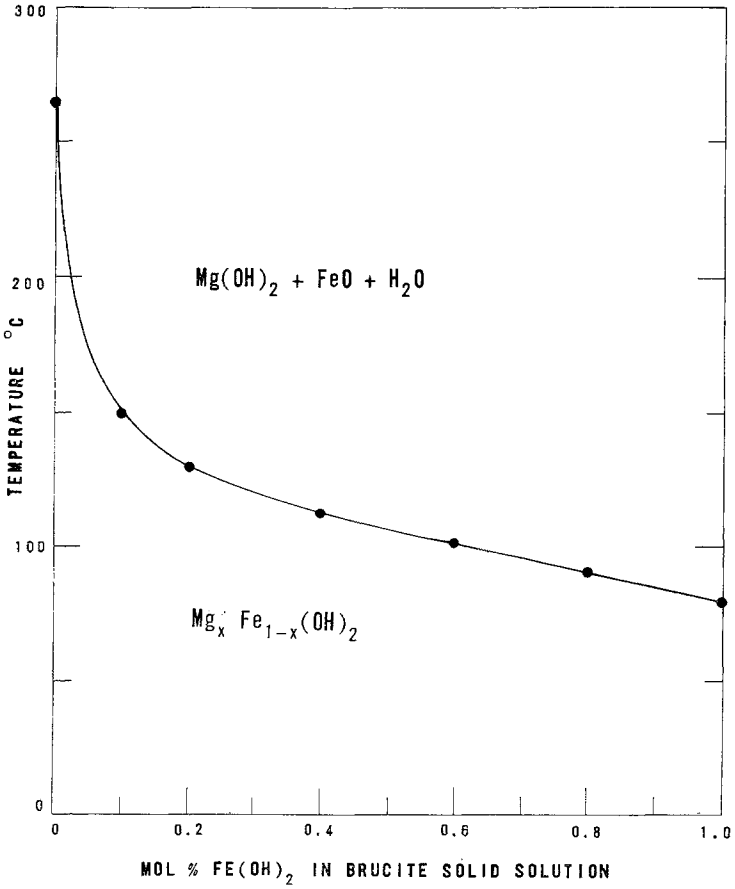

Fig. 9. Calculated temperature-composition diagram at 1 atmosphere pressure for brucite-$Fe(OH)_2$ solid solutions

ture. The calculations imply that reaction (2) takes place at much lower temperatures than suggested by the MgO-SiO_2-H_2O system.

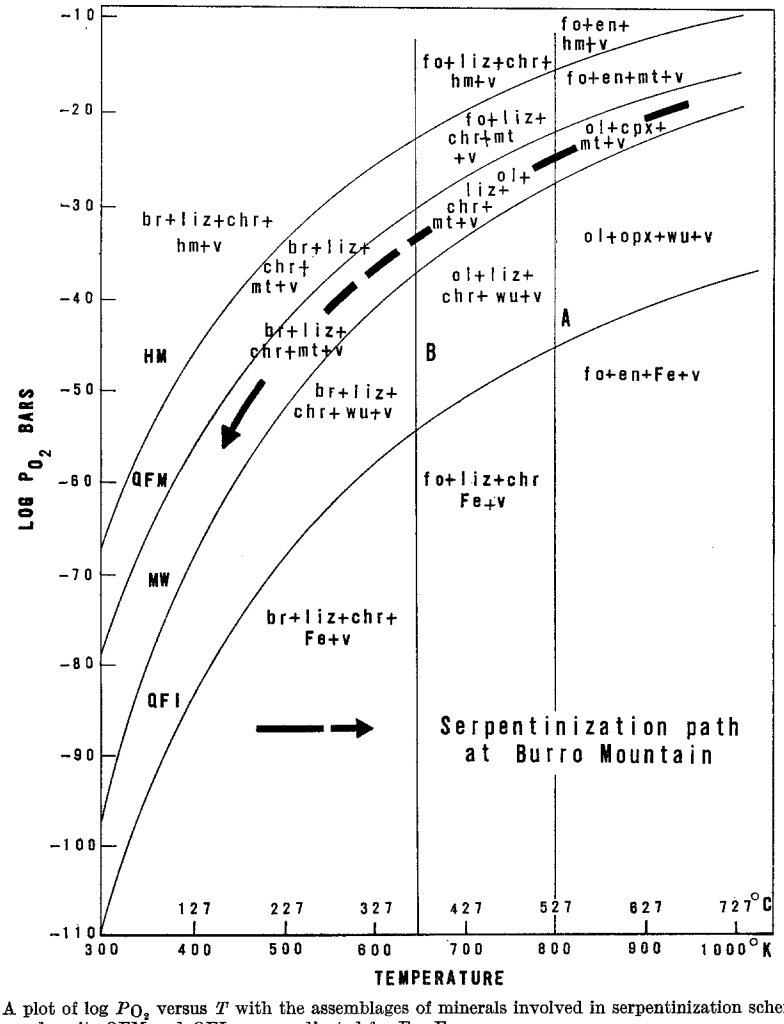

Fig. 10. A plot of log P_{O_2} versus T with the assemblages of minerals involved in serpentinization schematically superimposed on it. QFM and QFI curves adjusted for $Fo_{90}Fa_{10}$

Conclusions

The olivine, enstatite, and spinel from the peridotites and dunites of the Burro Mountain ultramafic complex altered to assemblages of chrysotile, lizardite, brucite, and magnetite. All of the assemblages originated in a changing P_{O_2}-T environment and are plotted schematically on a P_{O_2}-T section at a constant $P_{H_2O}=1$ kilobar (Fig. 10). The buffer curves of Fig. 10 were derived from WONES and EUGSTER (1965) by taking into account the dilution of fayalite by 90 mol percent forsterite. The position of lines A and B are not established, but are immaterial for representation of the various alteration assemblages. All of the possible phase assemblages are represented. Although various paths of serpentinization could produce the alteration assemblages at Burro Mountain, serpentinization probably proceeded along the heavy dashed curve. First, lizardite+chrysotile+magnetite were produced from olivine and enstatite, and later olivine altered to lizardite+chrysotile+brucite+magnetite.

Acknowledgments. Special thanks are due Professors W. S. FYFE, A. PABST, and H. HAWKES, who acted as advisors at the University of California, Berkeley, and to Dr. B. W. EVANS, of the University of California, who gave invaluable assistance in the microprobe work. The University also provided part of the financial support, which is gratefully acknowledged. R. G. COLEMAN, R. A. LONEY, and P. B. HOSTETLER, of the U. S. Geological Survey, gave generously of their time and offered many helpful suggestions during the research and in criticism of the manuscript. Core samples were donated by S. H. BURCH, of the U. S. Geological Survey.

References

BELL, G. L.: A geological section of the Santa Lucia Mountains, California. M. S. Thesis, University of California, Berkeley 1939.

BOWEN, N. L., and O. F. TUTTLE: The system MgO-SiO_2-H_2O. Bull. Geol. Soc. Am. **60**, 439—460 (1949).

BOYD, F. R.: Amphiboles. Carnegie Inst., Washington, Ann. Rept. Dir. Geophys. Lab., p. 108 (1954).

— Hydrothermal investigations of amphiboles. In: P. H. ABELSON (ed.), Researches in geochemistry, p. 377—396. New York: John Wiley & Sons, Inc. 1959.

BURCH, S. H.: Tectonic emplacement of the Burro Mountain ultramafic body, Southern Santa Lucia Range, California. Ph. D. Thesis, Stanford University, Stanford, California (1965).

BURNS, R. G.: Electronic spectra of silicate minerals: Application of crystal field theory to aspects of geochemistry. Ph. D. Thesis, University of California, Berkeley (1965).

FAIRBANKS, H. W.: Geology of northern Ventura, Santa Barbara, San Luis Obispo, Monterey, and San Benito Counties (California). California Mining Bur. 12th Rept. State Mineralogist, p. 493—526 (1894).

FYFE, W. S.: On the relative stability of talc, anthophyllite and enstatite. Am. J. Sci. **260**, 460—466 (1962).

GILLERY, G. H.: The X-ray study of synthetic Mg-Al serpentines and chlorites. Am. Mineralogist **44**, 143—152 (1959).

HILL, J. H.: The Los Burros District, Monterey County, California. U. S. Geol. Survey Bull. **735-J**, 323—329 (1923).

HOSTETLER, P. B., R. G. COLEMAN, F. A. MUMPTON, and B. W. EVANS: Brucite in alpine serpentinites. Am. Mineralogist **51**, 75—98 (1966).

KITAHARA, S., S. TAKENOUCHI, and G. C. KENNEDY: Phase relations in the system MgO-SiO_2-H_2O at high temperatures and pressures. Am. J. Sci. **264**, 223—233 (1966).

LATIMER, W. M.: The oxydation states of elements and their potentials in aqueous solutions, 392 p. New York: Prentice-Hall 1952.

NELSON, B. W., and RUSTUM ROY: Synthesis of chlorites and their structural and chemical compositions. Am. Mineralogist **43**, 707—725 (1958).

OLSEN, EDWARD: Equilibrium calculations in the system Mg, Fe, Si, O, H, and Ni. Am. J. Sci. **261**, 943—956 (1963).

PAGE, N. J.: Mineralogy and chemistry of the serpentine group minerals and the serpentinization process. Ph. D. Thesis, University of California, Berkeley (1966).

ROBIE, R. A.: Thermodynamic properties of minerals. U. S. Geol. Survey open-file rept., TEI-816 (1962).

ROY, D. M., and RUSTUM ROY: An experimental study of the formation and properties of synthetic serpentines and related layer silicate minerals. Am. Mineralogist **39**, 957—975 (1954).

— — Synthesis and stability of minerals in the system MgO-Al_2O_3-SiO_2-H_2O. Am. Mineralogist **40**, 147—178 (1955).

SEGNIT, E. R.: Synthesis of clinochlore at high pressures. Am. Mineralogist **48**, 1080—1089 (1963).

WHITNEY, J. D.: Report of progress and synopsis of the field work from 1860 to 1864. California Geol. Survey, Geology **1**, 498 (1865).

WHITTAKER, E. J. W., and J. ZUSSMAN: The characterization of serpentine minerals by X-ray diffraction. Min. Mag. **31**, 107—126 (1956).

WONES, D. R., and H. P. EUGSTER: Stability of biotite: experiment, theory and application. Am. Mineralogist **50**, 1228—1272 (1965).

YODER, H. S.: The MgO-Al_2O-SiO_2-H_2O system and the related metamorphic facies: Am. J. Sci. Bowen Vol., 569—627 (1952).

Dr. NORMAN J. PAGE
U. S. Geological Survey, Geologic Division, Branch of Astrogeology
345 Middlefield Rd., Menlo Park, Calif. 94025